Applied Optoelectronics in Medicine

Aplikovaná optoelektronika v lékařství

Interdisciplinary course at the CTU Prague (P317APL-E, W, 4 credits)

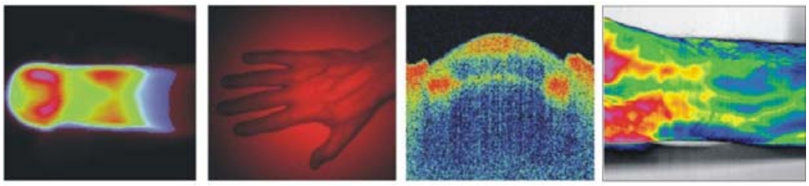

10. Optical imaging methods in medical diagnostics – part II
10. Optické zobrazovaci metody v lékařské diagnostice – část II

Learning aims of the tenth AOM lecture

- Photoplethysmography imaging (PPGI) – selected medical applications
- Optical coherence tomography (OCT)

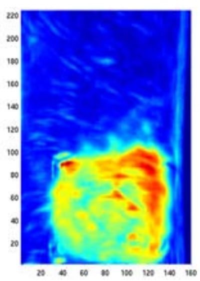

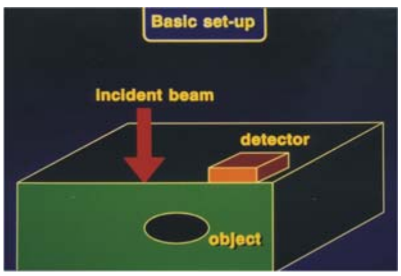

Photoplethysmography Imaging (PPGI) in clinical use

The first generation PPGI system in examination rooms of the University Hospital Aachen in a study for contactless functional quantification of skin perfusion

PPGI perfusion studies I:

first observation of "**blood volume clouds**" and their rhythmical movement in the skin

PPGI perfusion studies I:

first observation of
“blood volume clouds”
and their rhythmical
movement at the
forehead

a) One “moving” sensor
(32x32 Pixel = 1x1cm)

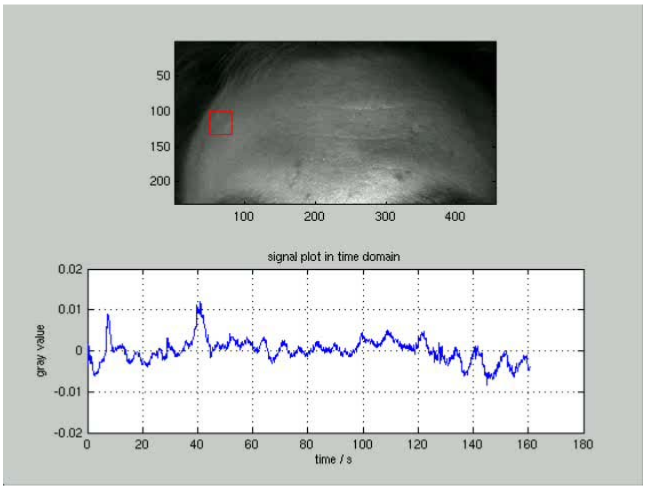

PPGI perfusion studies I:

first observation of
“blood volume clouds”
and their rhythmical movement
at the forehead

b) One sensor, different signal
processing
(16x16 Pixel = 5x5mm)

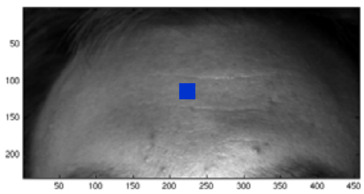

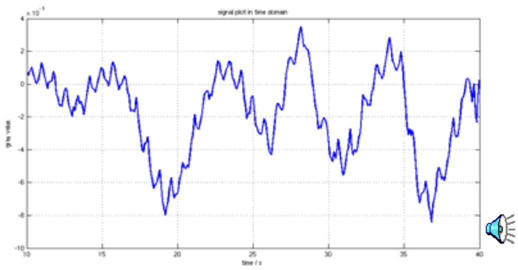

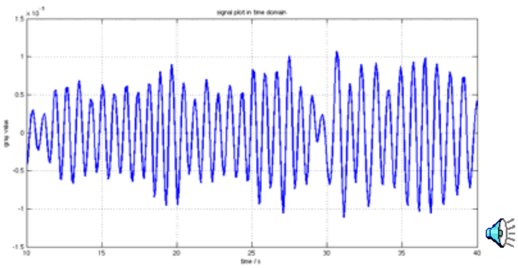

PPGI perfusion studies II: multidimensional perfusion analysis on the forehead

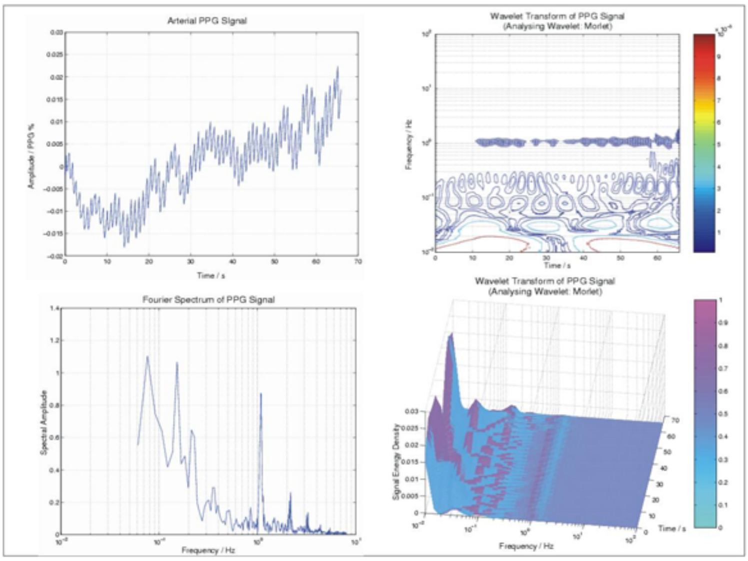

Fast Fourier transformation of quasi periodical perfusion signals

Benefit:
Spectral signal components can be visualized

Drawback:
Loss of time relation, inconclusive

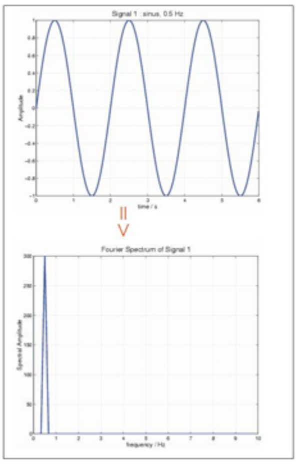

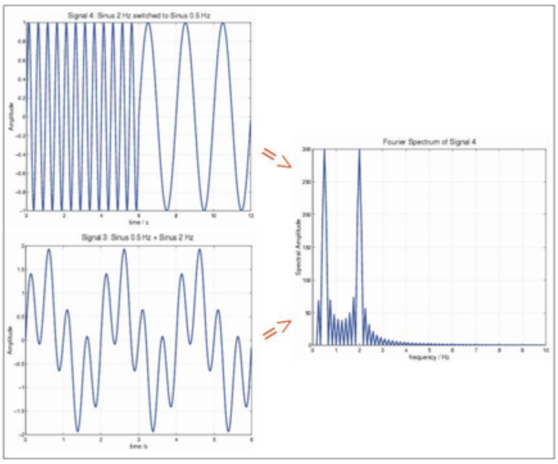

Wavelet transformation of quasi periodical perfusion signals

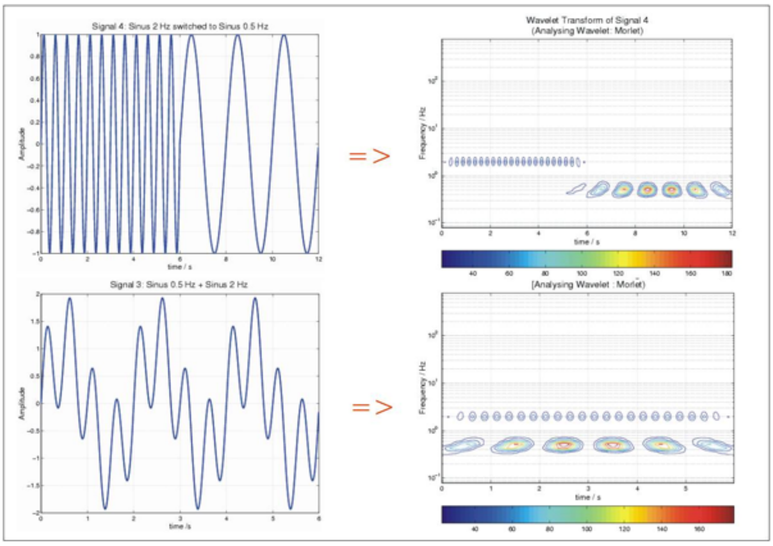

PPGI perfusion studies III:

measurements on the toes, artifact recognition

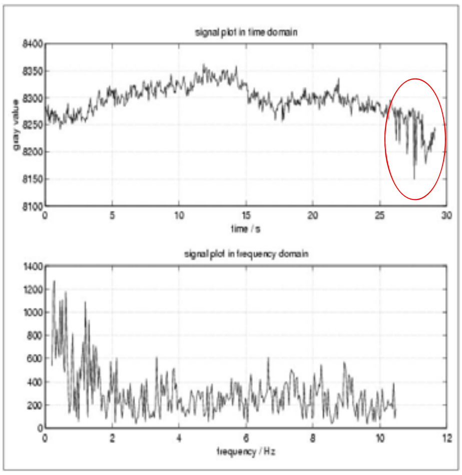

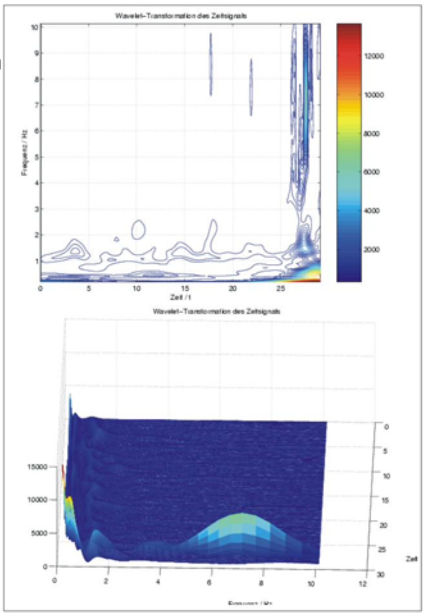

Remember:

- *The introduced WAVELET analysis of functional skin perfusion data offers new visualization possibilities in a multidimensional space;*
- *It combines the benefits of time-resolved and frequency-resolved monitoring of skin perfusion;*
- *An additional advantage is the possibility to recognize and to localize artifacts in the records;*
- *From physiological point of view the WA is "MATHEMATICAL MICROSCOPE*" for functional perfusion visualization;*
- *This procedure is also very powerful by visualization of quasi periodical phenomena (like earthquake, "el ninjo" and "tsunami" research)*

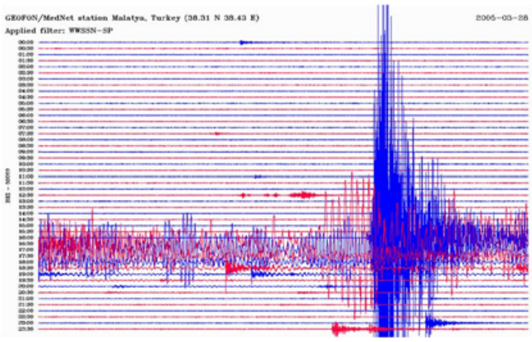

* Prof. Dr. Holger Schmid-Schönbein, Institute of Physiology, University Hospital RWTH Aachen

PPGI perfusion studies IV:

perfusion patterns in normal skin and wound areas

recorded skin regions

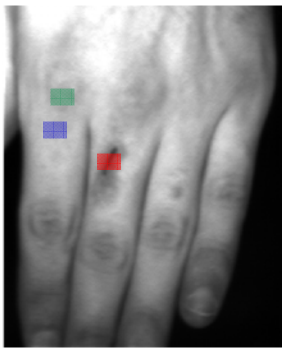

PPG signals in time and frequency domain

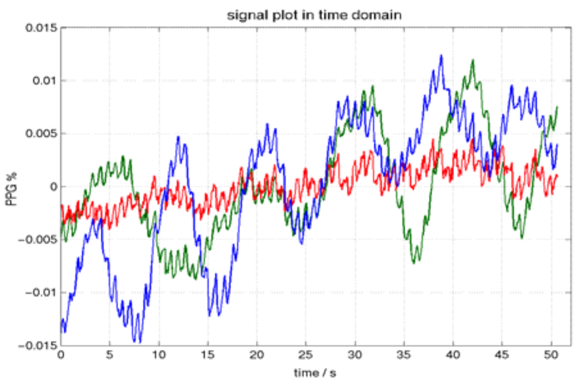

PPGI perfusion studies IV:

local variations in skin perfusion in the time and wavelet domain

healthy skin | healthy skin | wound

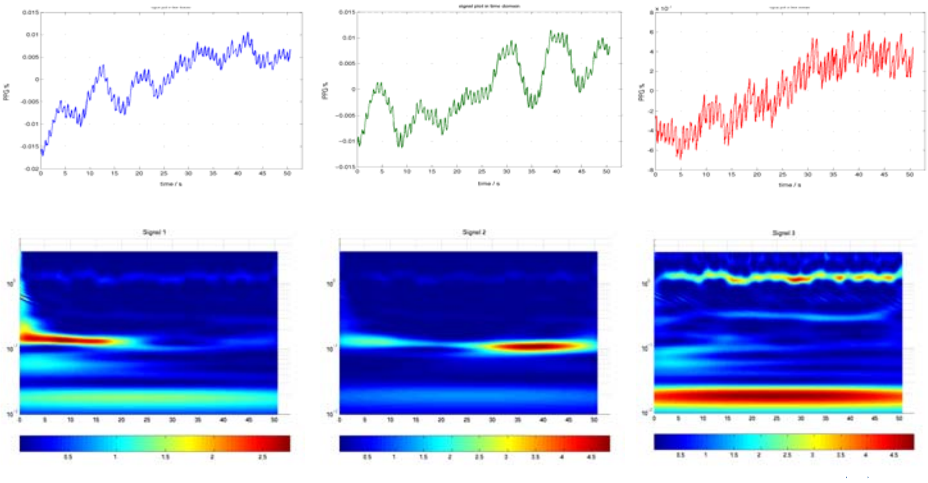

PPGI perfusion studies V:

perfusion changes inducted by local application of vasoactive salve & 2D visualisation

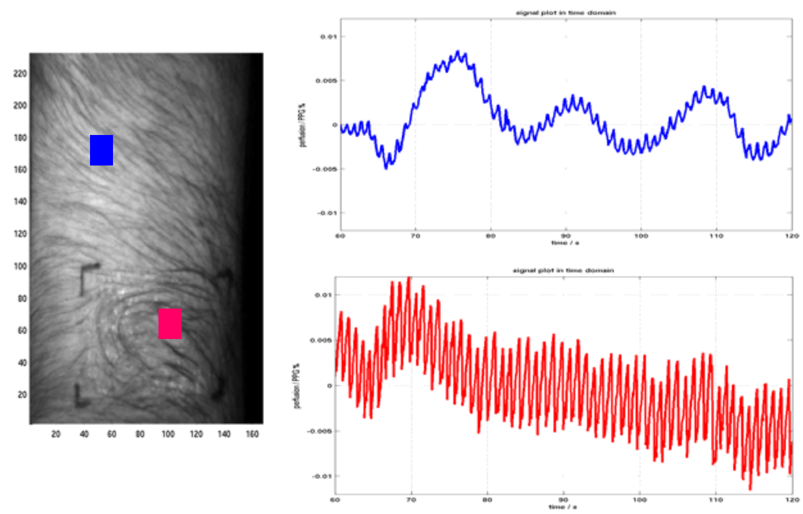

PPGI perfusion studies V:

perfusion changes inducted by local application of vasoactive salve & 2D visualisation

normal skin | treated skin

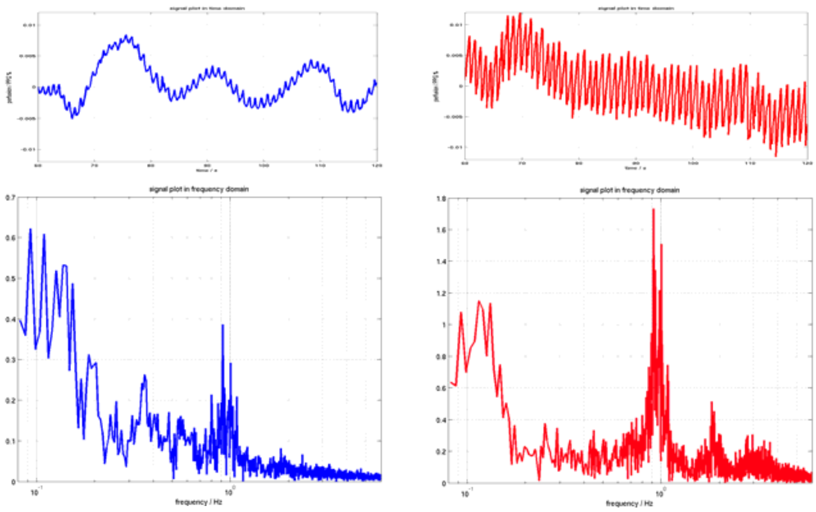

PPGI perfusion studies V: Calculation of „perfusion intensity“

PPG signal → bandpass filter f_1=0.6 Hz; f_2=2.5 Hz → total variation t.v. = $\sum | f(n) – f(n-1)|$

perfusion intensity / a.u.

healthy skin

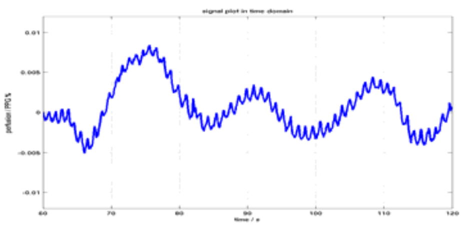

0.49

treated skin

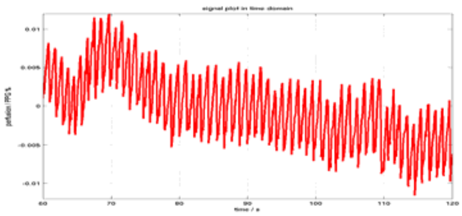

2.49

PPGI perfusion studies V: Signal post-processing and perfusion mapping

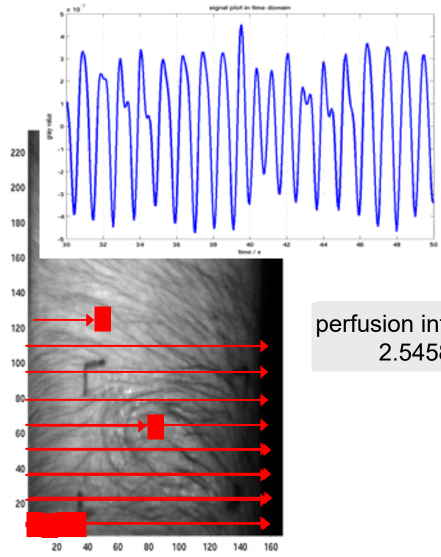

perfusion intensity:
2.5458

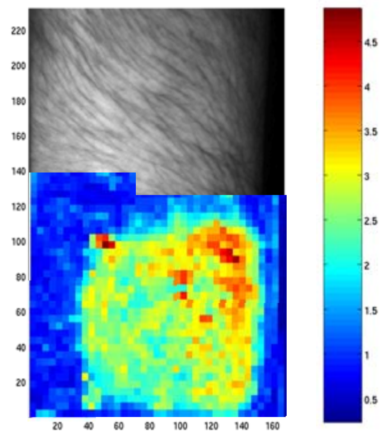

Remember:

The PPGI perfusion image does not depend on morphological but only on functional data

morphological image

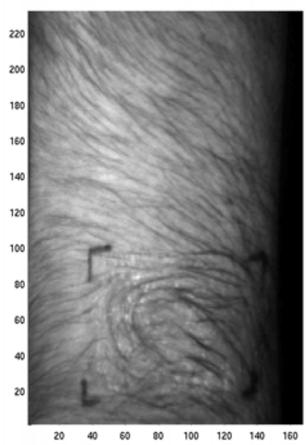

mapping of perfusion intensity

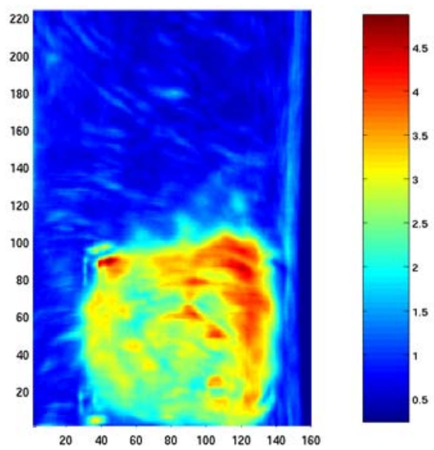

PPGI perfusion studies VI:

mapping of perfusion changes inducted by manual skin irritation (Demographometry)

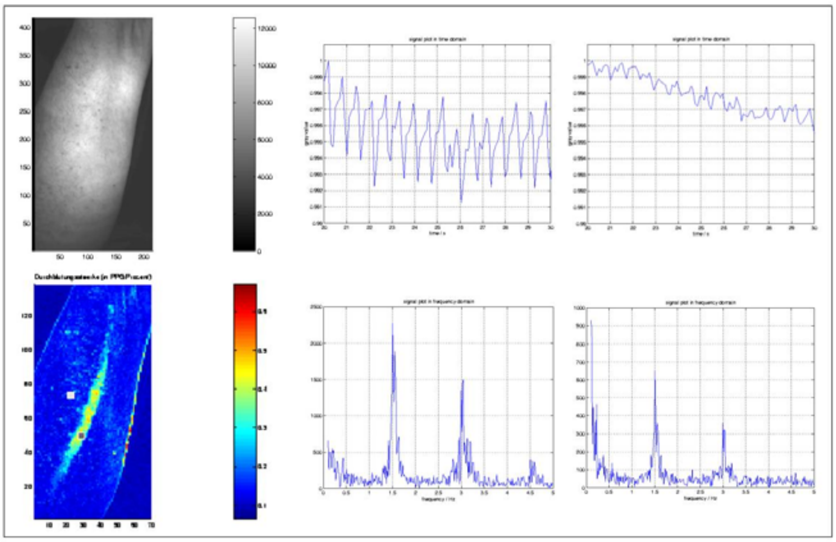

PPGI perfusion studies VII:

Functional testing of rapid class allergy in dermatology*

Design of the study:
Measurement area on the inner side of the lower arm

Size: ca. 100 x 200 mm
~ 128 x 256 Pixel

Spatial resolution: 0,78 mm

Temporal resolution: 12 fps

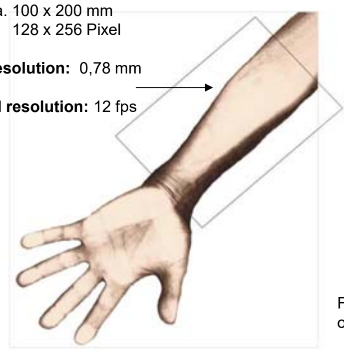

Measuring field 1: histamine prick, 1 drop local

Measuring field 2: NaCl prick, 1 drop local

Measuring field 3: histamine, 0,05ml i.c.

Four PPGI-sequences
of 2 minutes duration:

a) shortly before application
b) 4 minutes after application
c) 10 minutes after application
d) 16 minutes after application

Expected data volume
per patient:
650 MByte (1 CD)

* Blazek, C.R.: Some clinical applications of PPGI perfusion mapping in dermatology. In: Blazek, V., Rao, M.M., Kumar, V.J.: Kumar: Studies of skin perfusion dynamics - An overview of Indo-European research activities

PPGI perfusion studies VII:

Functional testing of rapid class allergy in dermatology*

Preliminary results:
Examination at one healthy control

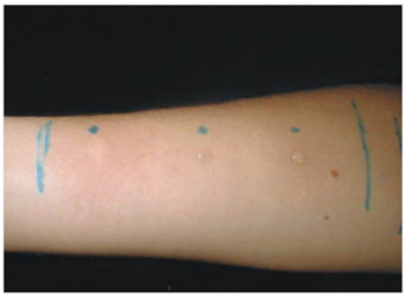

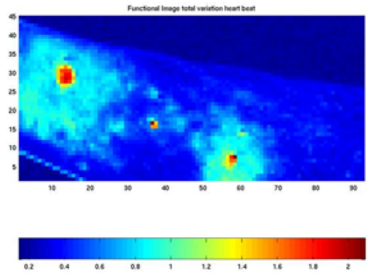

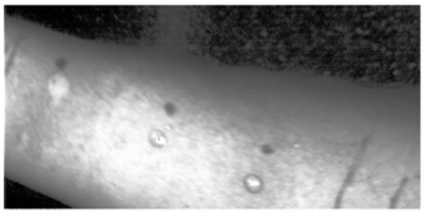

* Blazek, C.R.: Some clinical applications of PPGI perfusion mapping in dermatology. In: Blazek, V., Rao, M.M., Kumar, V.J.: Kumar: Studies of skin perfusion dynamics - An overview of Indo-European research activities

PPGI perfusion studies VII:

Functional testing of rapid class allergy in dermatology*

Preliminary results:
Examination at one healthy control

* Blazek, C.R.: Some clinical applications of PPGI perfusion mapping in dermatology. In: Blazek, V., Rao, M.M., Kumar, V.J.: Kumar: Studies of skin perfusion dynamics - An overview of Indo-European research activities

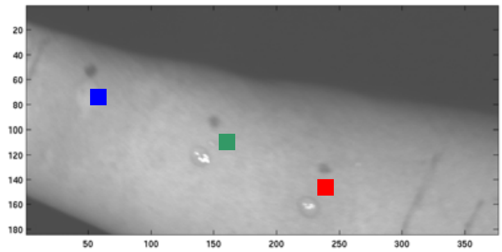

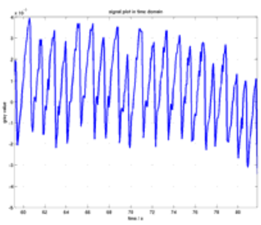

mean pulse amplitude = **0.45 PPG%**

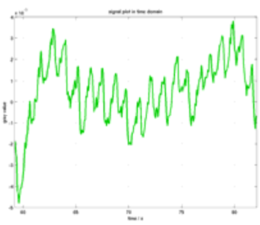

mean pulse amplitude = **0.2 PPG%**

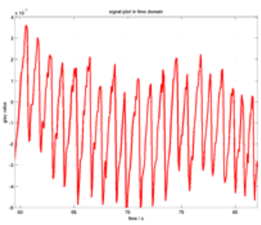

mean pulse amplitude = **0.5 PPG%**

PPGI perfusion studies VIII:
Contactless vital sign monitoring in neonatology

The time signal was calculated from the PPGI video stream for the red marked region of interest. The perfusion signal contains respiration components at 0.5 Hz as well as heart rate components at approx. 2 Hz.

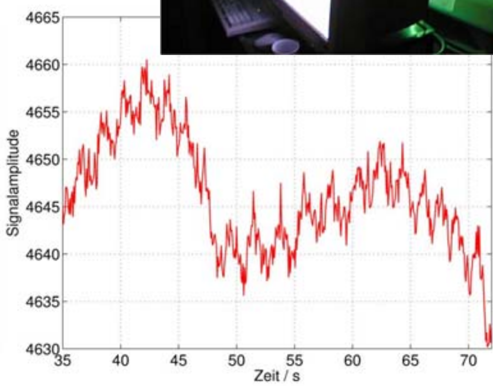

Vagades, J., Hülsbusch, M., Blazek, V., Poets, C.F.: Photoplethysmographisches Imaging (PPGI) - Erste Erfahrungen mit einer neuen Methode zur Haut-Perfusionsdiagnostik bei Frühgeborenen. Z. Geburtshilfe Neonatol 208 (2004),1055

Summary
PPGI opens a new dimension for quantification of heterogeneity of dermal perfusion and for experimental and clinical micro vascular perfusion studies during vasoactive therapy.

In contrast to LDPI, PPGI offers
- simultaneous perfusion registration in all image points (camera instead of scanning)
  - higher resolution

50 x 50 µm

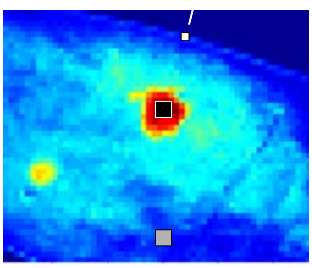

15 fps

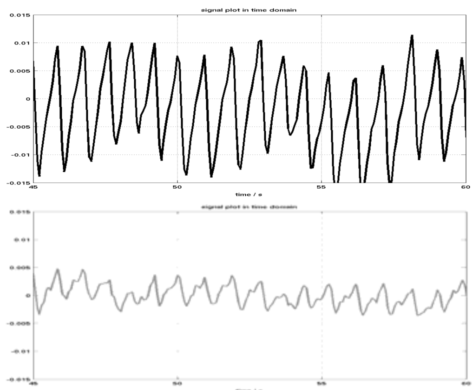

Optical coherence tomography (OCT)

Goal: destruction and stress-free, skin depth resolved visualization of tissue structure by time-resolved detection of scattered optical signal

OCT is an optical signal acquisition and processing method. It captures micrometer-resolution, three-dimensional images from within optical scattering media (e.g., biological tissue). It is an interferometric technique, typically employing near-infrared light. The use of relatively long wavelength light allows it to penetrate into the scattering medium. Starting from white-light interferometry for *in vivo* ocular eye measurements imaging of biological tissue, especially of the human eye, was investigated by multiple groups worldwide. A first two-dimensional *in vivo* depiction of a human eye fundus along a horizontal meridian based on white light interferometric depth scans was presented in 1990. Further developed in 1990/91 OCT with micrometer resolution and cross-sectional imaging capabilities has become a prominent biomedical tissue-imaging technique; it is particularly suited to ophthalmic applications and other tissue imaging requiring micrometer resolution and millimeter penetration depth. First *in vivo* OCT images – displaying retinal structures – were published in 1993.OCT has critical advantages over other medical imaging systems. Light in an OCT system is broken into two arm, a sample arm (biotissue probe) and a reference arm (usually a mirror). The combination of reflected light from the sample arm and reference light from the reference arm gives rise to an interference pattern, but only if light from both arms have travelled the "same" optical distance ("same" meaning a difference of less than a coherence length).

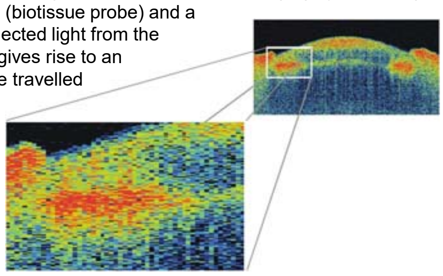

OCT implementation approaches:

- Use of ultra short pulses
- Utilization of limited coherence lengths
- Frequency coding of the laser probe beam

Optical coherence tomography (OCT)

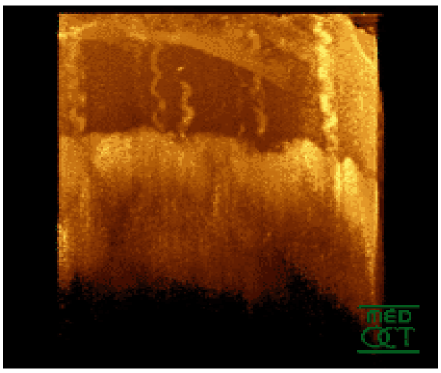

Rotating image of OCT tomogram of a fingertip, depicting stratum corneum (~500µm thick) with stratum disjunctum on top and stratum lucidum (connection to stratum spinosum) in the middle. At the bottom are superficial parts of the dermis. Sweatducts are clearly visible. This animated image loads 85x times slower than the non-animated image.

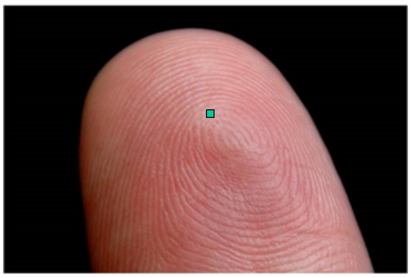

Classical digital image of the investigated skin area

http://en.wikipedia.org/wiki/Optical_coherence_tomography

OCT implementation option 1:
ultra short pulse setup

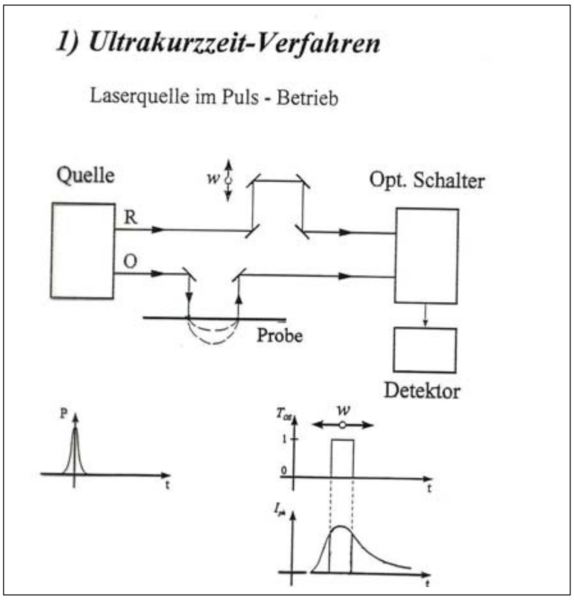

OCT implementation option 2:
low coherence setup

After initial experiments with light sources limited bandwidth (a few nm) were relatively broad-band light sources available and used with high spatial coherence. In most cases, the OCT systems on superluminescent diodes with a few tens of nanometers bandwidth (typically 50 nm, equivalent to more than 50 microns resolution). Firs in the 1997 the leap from that standard resolution is successfully ventured up to the "ultra high resolution" (LED bandwidth > 100 nm, corresponding to less than 3 microns axial tissue resolution).
The OCT tomograms allows today structure resolutions almost comparable with histological sections.

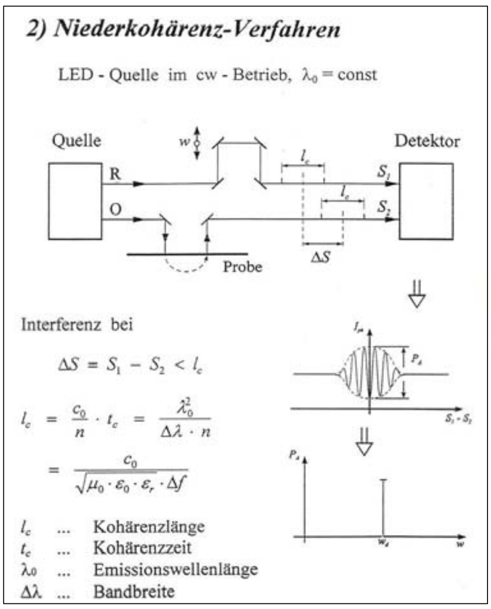

Axial OCT resolution (stand 2005)

at a varying bandwidth and central wavelength for different light sources

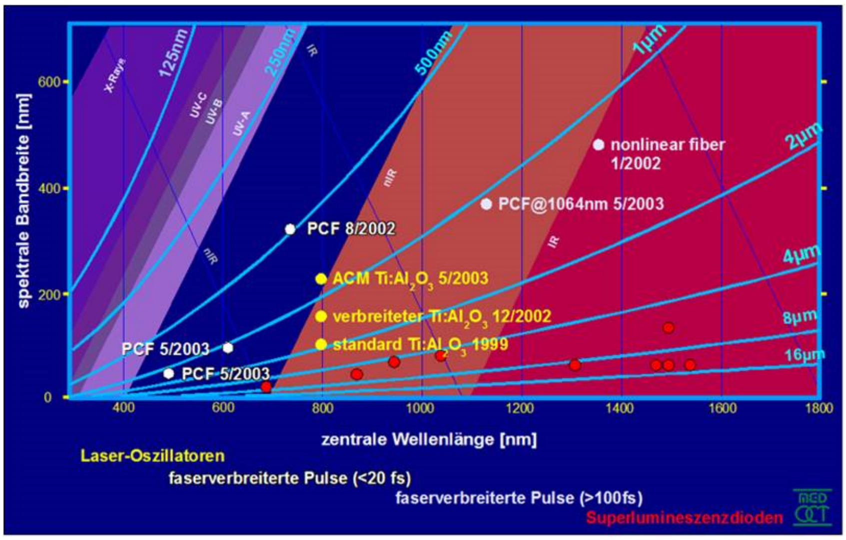

Quelle: medOCT-Gruppe, Zentrum für biomedizinische technik und Physik, Med. Univ. Wien, Austria, 2005 http://de.wikipedia.org/wiki/Optische_Kohärerenztomografie

High resolution low coherence OCT - experimental setup by Fujimuto, MIT

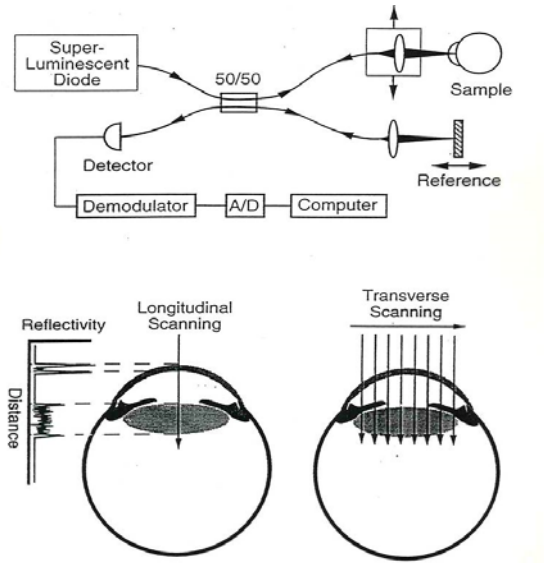

RESEARCH LABORATORY OF ELECTRONICS AT MIT

High resolution low coherence OCT
by Fujimuto, MIT

$$\Delta z = \frac{2\ln(2)\,\lambda_0^2}{\pi\,\Delta\lambda}$$

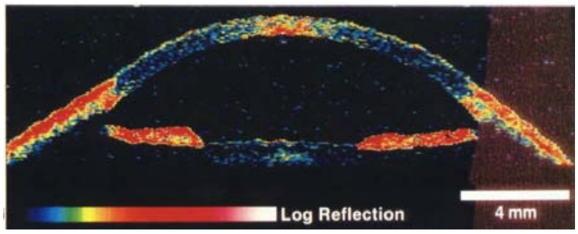

In vivo OCT scan of a retina at 800 nm (λ_0) and an axial resolution Δz of 3 microns (!)

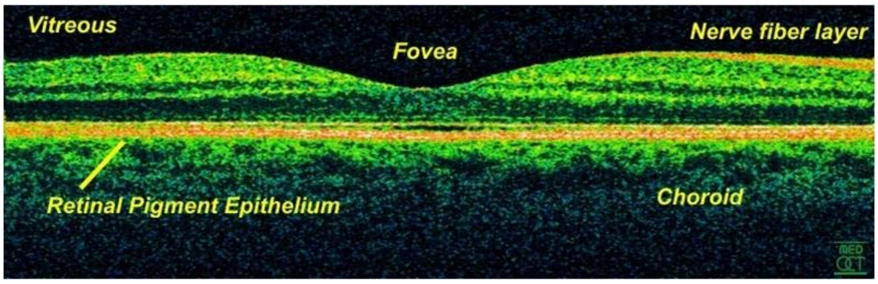

http://de.wikipedia.org/wiki/Optische_Kohärerenztomografie

OCT instrument STRATUSOCT ™ from Zeiss for retinal diagnostics

The system provides cross-sectional images of retinal tissue layers in never before seen accuracy and allows the physician a non-invasive quantitative imaging of internal retinal structures.

Quelle: www.meditec.zeiss.de

OCT instrument STRATUSOCT ™ from Zeiss for retinal diagnostics

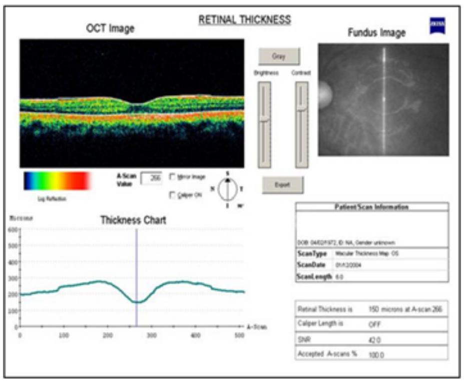

Retinal thickness (one eye) along the scan lines obtained at the macula

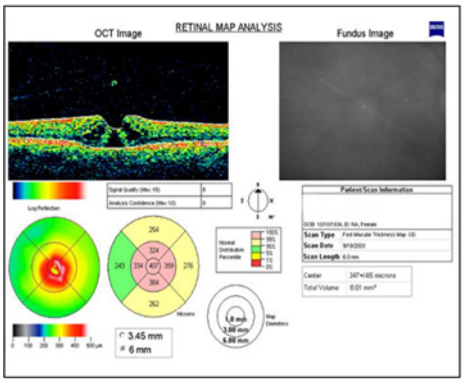

Retinal probability map (both eyes) using a 5-color-coding and the other shows the numerical deviation from the patient's eye to normative mean value.

Quelle: www.meditec.zeiss.de

OCT tomogram of skin melanoma on thigh (in vitro)

Left: Melanoma in enlarged epidermis with increased backscattering in the upper part of the frame. Inside the melanoma (A-scan) increased homogeneous scattering signals, epidermal thickness 400 mm. In the area of healthy skin (B-Scan) individual skin layers clearly visible.

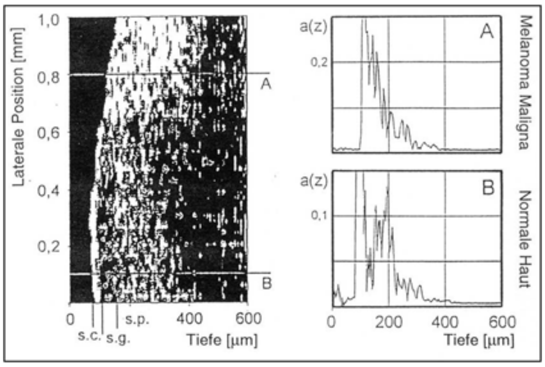

Histological comparison cuts

Left: section through the healthy skin
Right: section of melanoma in the epidermis

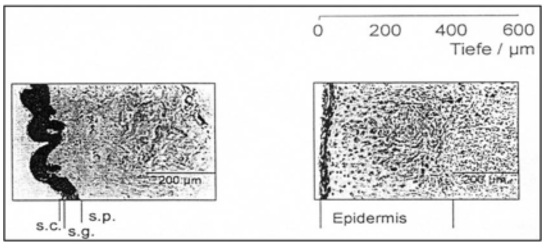

Results from Häusler et al., University of Erlangen, Germany

Excursus

RF ultrasonic tomogram (50 MHz)
a benign (above) and
a malignant (bottom)
tumor

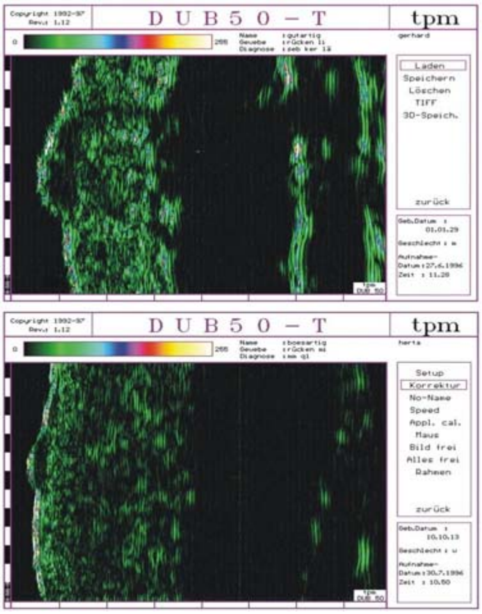

Source: Perimed, Schweden

Excursus

Penetration and structural resolution of the ultrasonic tomography

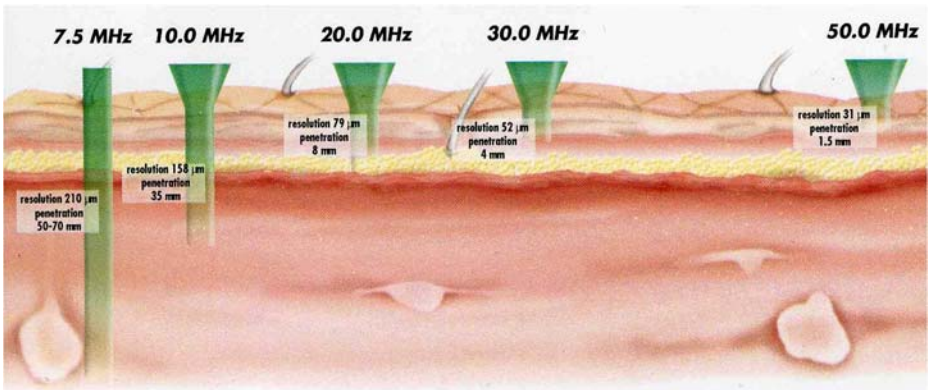

Quelle: Perimed, Schweden

Low coherence optical tomography in transillumination mode

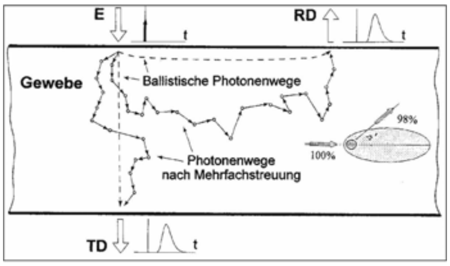

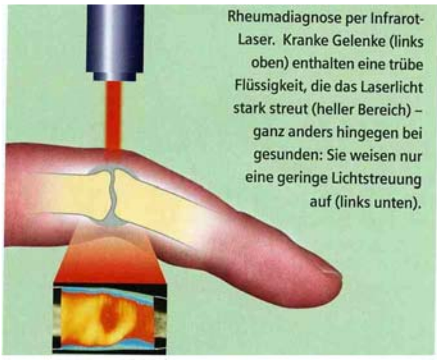

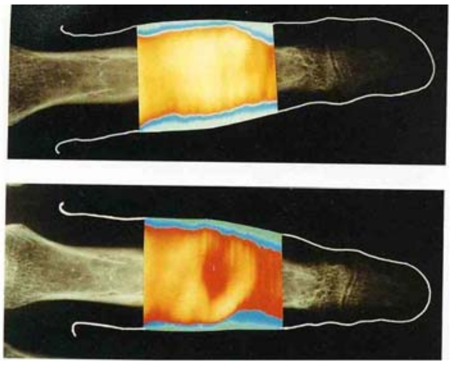

Low coherence optical mammography

measuring setup

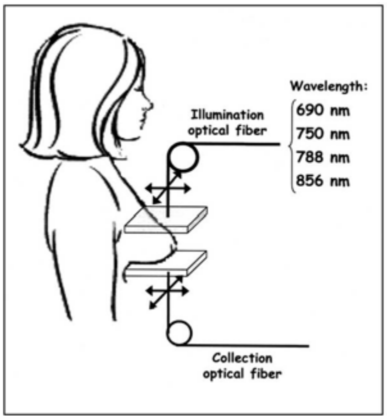

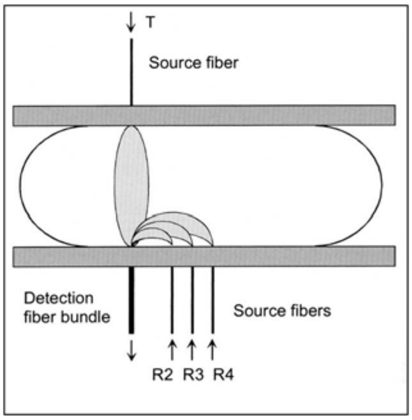

Heffer et al.: Near-infrared imaging of the human breast. Journal of Biomedical Optics 9 (2004), 1152-1160

Low coherence optical mammography: published high resolution tomogramms

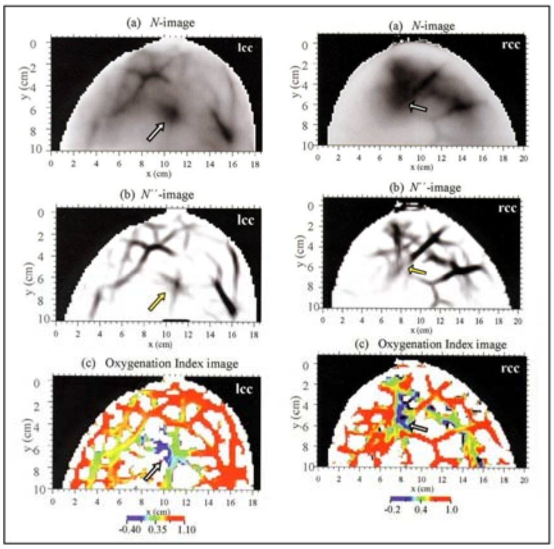

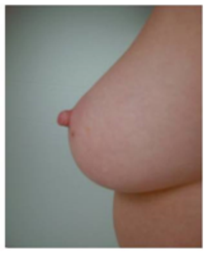

Heffer et al.: Near-infrared imaging of the human breast.
Journal of Biomedical Optics 9 (2004), 1152-1160

OCT implementation option 3:

Frequency coding laser setup (Chirp)

Chirp OCT is based on a continuous wave frequency modulated radar, but uses a tunable laser in the near infrared. As the full width at half maximum resolution of 16 mm is demonstrated with an external cavity laser, the chirp OCT becomes an alternative to conventional short coherence tomography with the advantage of a simplified optical setup.

Remember:

As a chirp (chirping of a cicada) refers to a signal whose frequency varies with time

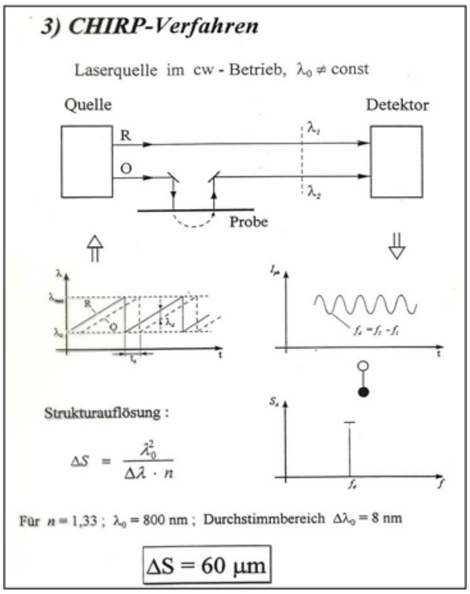

U. H. P. Haberland, V. Blazek, and H. J. Schmitt:Chirp optical coherence tomography of layred scattering media. Journal of Biomedical Optics 3 (1998), pp. 259-266

CHIRP-OCT-Vorbild: FMCW Radar mit einem linearen Chirp

Für den Spezialfall eines linearen Chirp steigt die Frequenz linear mit der Konstanten *k* an:

$f(t) = f_0 + kt$ und es gilt für den Zeitverlauf *x(t)*:

$$x(t) = \sin(2\pi \int_0^t f(t')\, dt') = \sin(2\pi \int_0^t (f_0 + kt')\, dt') = \sin\left(2\pi(f_0 + \frac{k}{2}t)t\right).$$

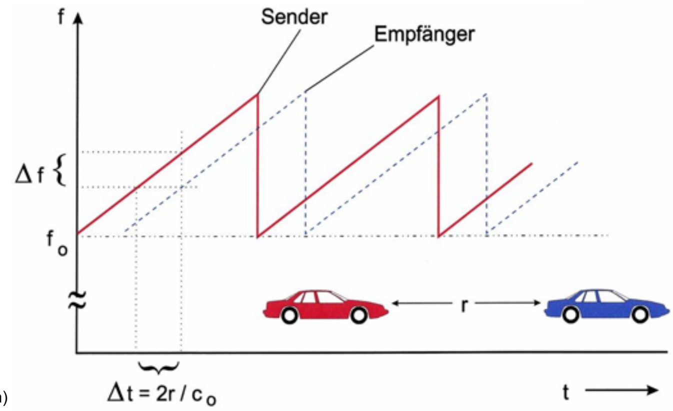

Sound 1:
Akustisches Beispiel eines
linearen Chirps (5 Wiederholungen)

Sound 2: In für das menschliche Ohr hörbare Laute umgewandelte Ultraschall-Rufe jagender Fledermäuse

CHIRP OCT:

Block diagram and operating principle of the RWTH measurement concept, the core of which is a linearly tunable laser and a Michelson interferometer

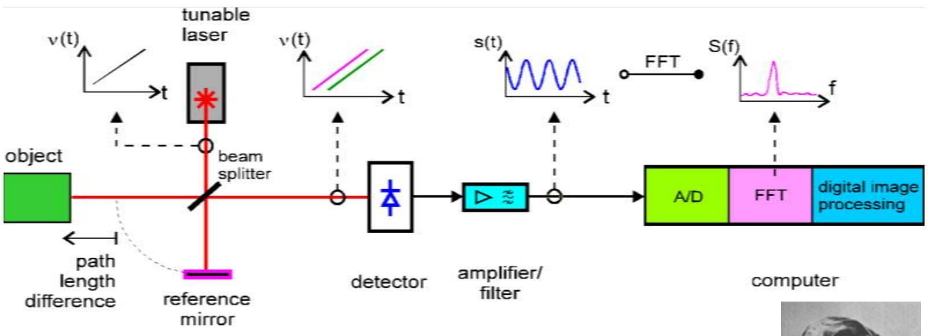

The **Michelson interferometer** is the most common configuration for optical interferometry and was invented by Albert Abraham Michelson (1852 – 1931). An interference pattern is produced by splitting a beam of light into two paths, bouncing the beams back and recombining them. The different paths may be of different lengths or be composed of different materials to create interference fringes on a back detector.
In 1907 Prof. Michelson was awarded with the Nobel Prize in Physics.

Tuning principles for the coherent CHIRP light source

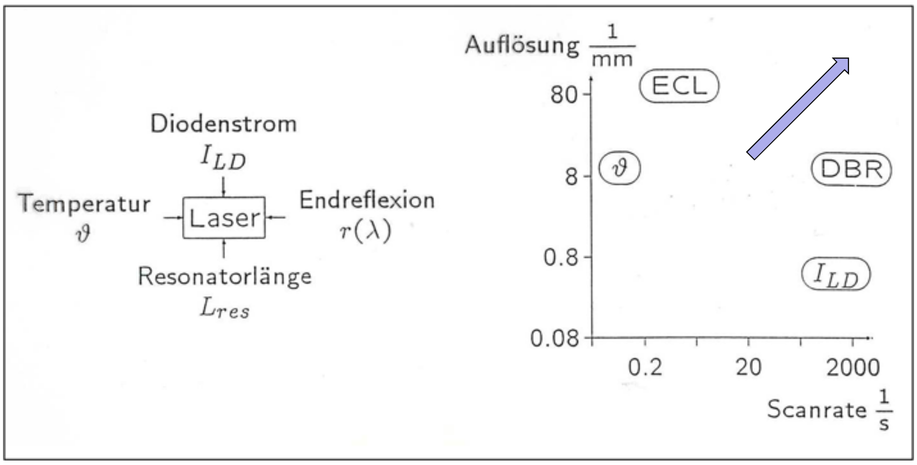

Former OCT laboratory at the IHF / RWTH Aachen University

CHIRP OCT results (anno 2000)

Imaging of scattering phantoms

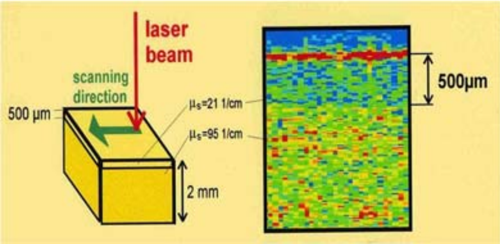

Axial resolution image taken
a foil by vertical illumination

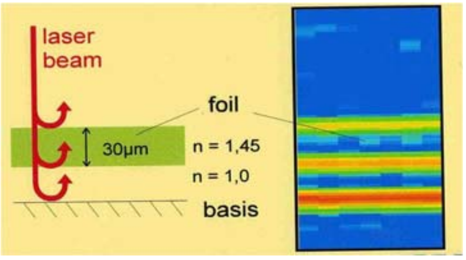

CHIRP OCT results (anno 2000)

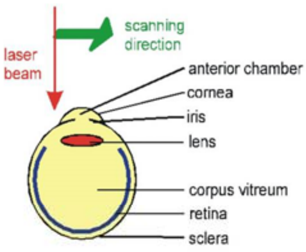

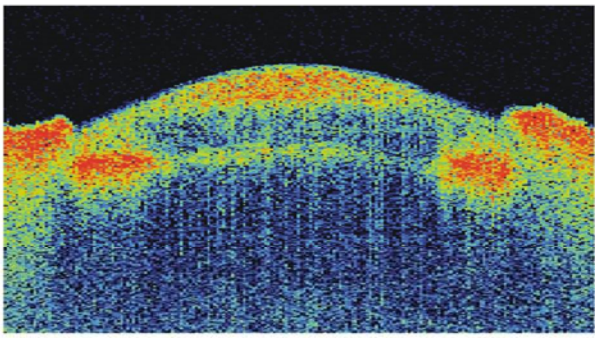

Objekt	vordere Augenkammer	Linse	Glaskörper	Gesamtlänge
Auge 1	4,1 mm	4,4 mm	18,7 mm	27,2 mm
Auge 2	4,2 mm	4,4 mm	19,5 mm	28,1 mm

CHIRP OCT: Morphology & velocity imaging

Measuring scenario:

Solid scattering phantom with a hole of diameter 3 mm drilled 5 mm underneath the surface.
A scattering liquid (diluted milk) was running through the pipe at a constant flow.

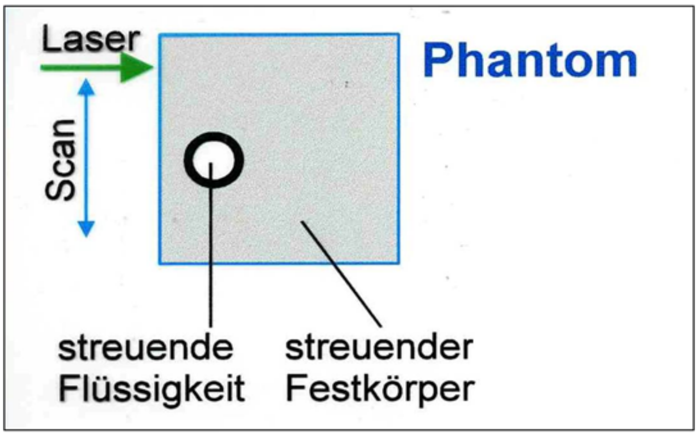

OCT: Morphology & velocity imaging

Measuring scenario:

Solid scattering phantom with a hole of diameter 3 mm drilled 5 mm underneath the surface.
A scattering liquid (diluted milk) was running through the pipe at a constant flow.

Lateral resolved laser Doppler perfusion map (constant flow of 0.77 ml/min; v_{max}= 3.6 mm/s)

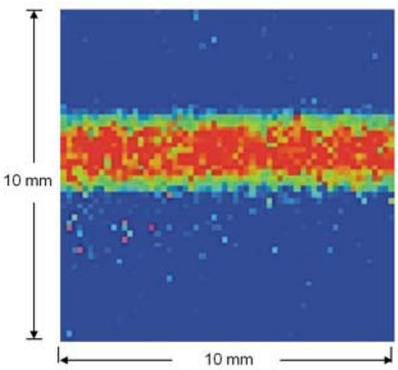

Functional cross sectional (depth resolved) images

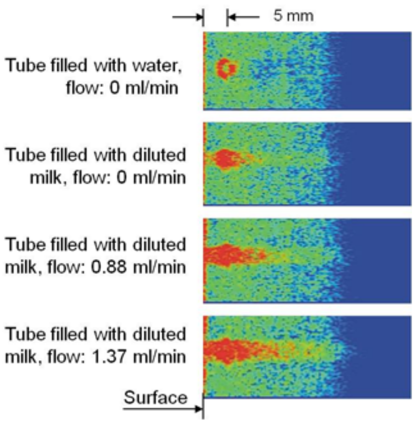

OCT: Morphology & velocity imaging

Combined up/down-chirp sequences with DOPPLER break

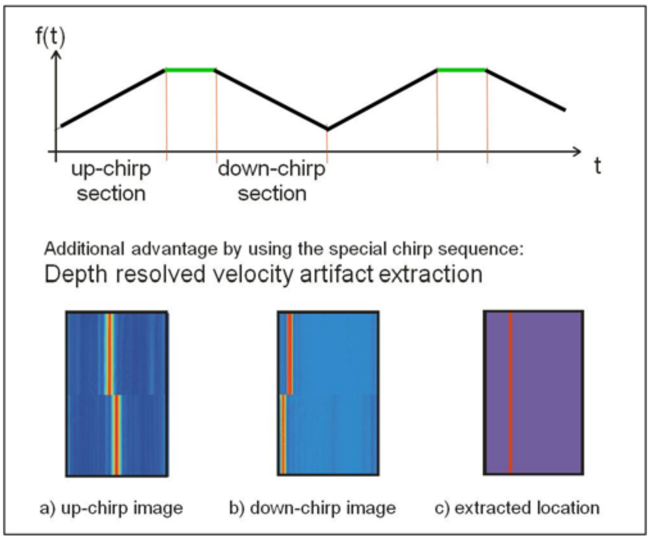

Optical coherence tomography

… development of research papers in
selected scientific journals …

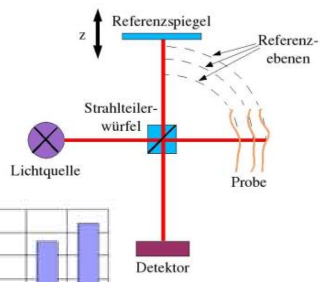

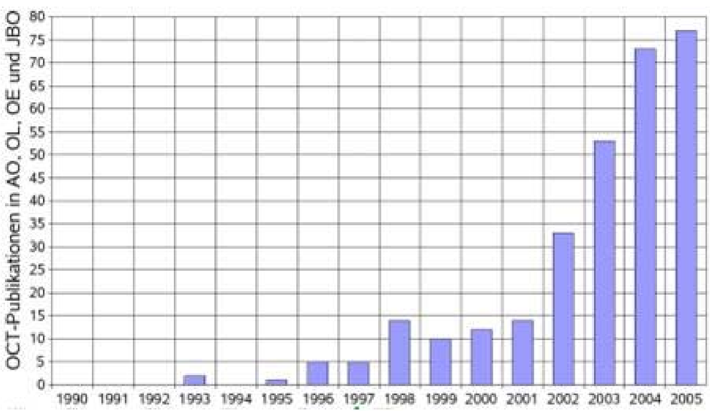

Recommended for further studies:

Top 8 OCT publications in major international peer-reviewed journals

W. Drexler, J.G. Fujimoto: State-of-the-art retinal optical coherence tomography. *Prog Retin Eye Res*, 27(1):45-88, 2008

W. Drexler: Cellular and Functional Optical Coherence Tomography of the Human Retina, The Cogan Lecture, *Invest. Opthalmol. Vis. Sci.* 48 (12): 5340-5351, 2007

K. Bizheva, R. Pflug, B. Hermann, B. Povazay, H. Sattmann, E. Anger, H. Reitsamer, S. Popov, J.R. Tylor, A. Unterhuber, P. Qui, P.K. Ahnlet, W. Drexler. Optophysiology: depth resolved probing of retinal physiology with functional ultrahigh resolution optical coherence tomography. *PNAS* 103(13):5066-71, 2006

U. Schmidt-Erfurth, R.A. Leitgeb, S. Michels, B. Povazay, S. Sacu, B. Hermann, H. Sattmann, C. Scholda, A.F. Fercher, W. Drexler: Three-dimensional ultrahigh resolution optical coherence tomography of macular pathologies. *Invest. Ohthalmol. Vis. Sci.*, 46(9):339302, 2005

U.J. Hermann, A. Fernández, H. Unterhuber, A.F. Sattmann, A.F. Fercher, W. Drexler, P.M. Prieto, P. Artal: Adaptive optics ultrahigh resolution optical coherence tomography. *Optics Letters* 29(18):1-3, 2004

W. Drexler: Ultrahigh resolution optical coherence tomography. *J Biomed Optics*, 9(1):47-74, 2004

W. Drexler, H. Sattmann, B. Hermann, T.H. Ko, M. Stur, A. Unterhuber, C. Scholda, O. Findl, M. Wirtitsch, J.G. Fujimoto, A.F. Fercher: Enhanced visualization of macular pathology using ultrahigh resolution optical coherence tomography. *Arch Opthalmol*, 121(5):695-706, 2003

A. Unterhuber, B. Hermann, H. Sattmann, B. Povazay, W. Drexler, G. Tempea, V. Yakovlev, C. Schubert, E.M. Anger, P.K. Ahnelt, M. Stur, J.E. Morgan, T. Le, A. Stingl: Compact, low cost Ti:Al2O3 laser for in vivo ultrahigh resolution optical coherence tomography. *Optics Lett*ers 28(11):905-7, 2003

Instead of conclusion I:

A radical shift in thinking about modern diagnostic techniques in medicine

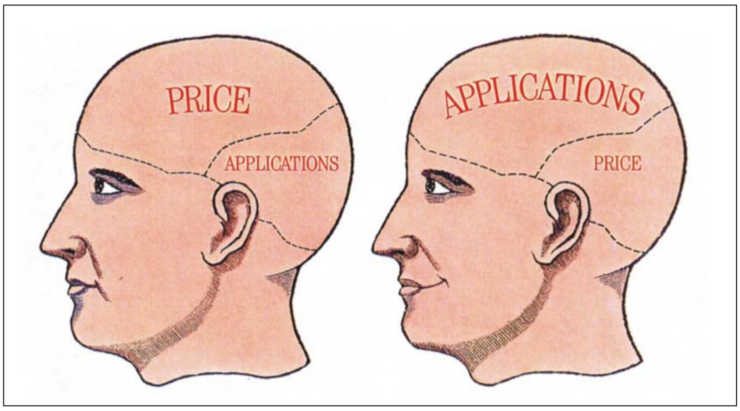

Instead of conclusion II:

Thanks for listening
and active participation …

Citát pro desátou přednášku / Quotation of the lecture 10:

“Wo wenig Licht ist, da ist auch wenig Schatten”

Das zweitpopulärste Zitat von Götz von BERLICHINGEN (1480 – 1562)